PHYSICAL REVIEW E **83**, 020401(R) (2011)

Shear-induced criticality near a liquid-solid transition of colloidal suspensions

Masamichi J. Miyama and Shin-ichi Sasa
Department of Pure and Applied Sciences, University of Tokyo, Komaba, Meguro-ku, Tokyo 153-8902, Japan
(Received 7 October 2010; published 15 February 2011)

We investigate colloidal suspensions under shear flow through numerical experiments. By measuring the time-correlation function of a bond-orientational order parameter, we find a divergent time scale near a transition point from a disordered fluid phase to an ordered fluid phase, where the order is characterized by a nonzero value of the bond-orientational order parameter. We also present a phase diagram in the $(\rho,\dot{\gamma}^{\rm ex})$ plane, where ρ is the density of the colloidal particles and $\dot{\gamma}^{\rm ex}$ is the shear rate of the solvent. The transition line in the phase diagram terminates at the equilibrium transition point, while a critical region near the transition line vanishes continuously as $\dot{\gamma}^{\rm ex} \to 0$.

DOI: 10.1103/PhysRevE.83.020401 PACS number(s): 82.70.−y, 64.60.Cn, 83.10.Mj, 83.50.Ax

I. INTRODUCTION

A crystal phase is distinguished from a liquid phase by a translational and rotational symmetry breaking in space. Since there exists an order parameter associated with the symmetry breaking, the nature of the transition to a crystal phase is rather different from that of gas-liquid transitions, although both are first-order transitions from the viewpoint of thermodynamics. In short, the transition to a crystal phase is classified as a symmetry-breaking first-order transition.

The correlation time of fluctuations does not diverge near symmetry-breaking first-order transitions. This is in sharp contrast to the case of a symmetry-breaking second-order transition, which exhibits a divergent time scale when approaching a liquid gas critical point. On the basis of standard understanding, in this paper, we argue that a divergent time scale of steady-state fluctuations may appear near an equilibrium crystallization (symmetry-breaking first-order transition) point when a nonequilibrium condition is imposed.

Concretely, we study colloidal suspensions under shear flow through numerical experiments. Since the pioneering work by Ackerson and Clark [1], there have been extensive studies related to the crystallization of colloidal suspensions under shear flow [2–6]. In particular, a phase diagram was obtained by numerical experiments [2] and laboratory experiments [3], together with numerical realizations of crystal-liquid coexistence under shear flow [4]. In order to clarify the microscopic mechanism for the transition to a crystal, the kinetics of homogeneous nucleation under shear flow was also investigated [5]. However, to our knowledge, shear-induced criticality near an equilibrium crystallization point has never been reported, except for our preliminary observation [6].

In this study, we focus on time scales associated with the relaxation from a bond-orientational ordered state in a disordered regime. We first note that the relaxation time, even in equilibrium cases, diverges near the melting point [7,8]. We characterize the parameter dependence of the relaxation time quantitatively by measurement of the time series of a bond-orientational order parameter. The result is well fitted by the Vogel-Fulcher law, which suggests the existence of a nucleation process of disordered fluid regions in a crystal state. However, since crystals do not appear spontaneously in the disordered phase, the divergent time scale has never been observed in steady-state fluctuations. In contrast, in nonequilibrium systems under shear flow, the relaxation time exhibits a power-law divergence near a transition point to an ordered fluid, which suggests the existence of critical slowing down. The power-law divergent time scale is also observed in steady-state fluctuations. We refer to this phenomenon as *shear-induced criticality near a liquid-solid transition*.

II. MODEL

We investigate N colloidal particles that are suspended in a solvent fluid confined to an $L \times L \times L$ cubic box. We impose planar Couette flow on the solvent and choose the x and z axes to be the directions of the shear velocity and the velocity gradient, respectively. Concretely, the velocity profile of the solvent is assumed to be given as $(\dot{\gamma}^{\rm ex}z,0,0)$. We impose periodic boundary conditions along the x and y axes and introduce two parallel walls so as to confine particles in the z direction. Let $\boldsymbol{r}_i$, $i = 1,\ldots,N$, be the position of particle i. The potential energy of particles $U(\{\boldsymbol{r}_j\}_{j=1}^N)$ consists of two parts: $\sum_{i<j} U^{\rm LJ}(|\boldsymbol{r}_i - \boldsymbol{r}_j|)$ and $\sum_i U^{\rm wall}(\boldsymbol{r}_i)$. The former describes the interaction potential among particles, where $U^{\rm LJ}(r) = 4\epsilon[(\sigma/r)^{12} - (\sigma/r)^6] - U_{\rm cutoff}$ for $r < r_{\rm c}$ with cutoff length $r_{\rm c}$ and $U_{\rm cutoff} = 4\epsilon[(\sigma/r_{\rm c})^{12} - (\sigma/r_{\rm c})^6]$, while $U^{\rm LJ}(r) = 0$ otherwise. $U^{\rm wall}(\boldsymbol{r}_i)$ represents the wall potential and is given by $U^{\rm wall}(\mathbf{r}_i) = u^{\rm WCA}(r^* - L/2 \pm z_i)$ for $L/2 \pm z_i < r^*$ with the Weeks-Chandler-Andersen potential $u^{\rm WCA}$ [9], while $U^{\rm wall}(\boldsymbol{r}_i) = 0$ otherwise. We define momentum of the ith particle relative to the shear flow as $\boldsymbol{p}_i(t) \equiv m\dot{\boldsymbol{r}}_i(t) - m\dot{\gamma}^{\rm ex}z_i(t)\boldsymbol{e}_x$, where m is the mass of a single particle. We then assume the equation of motion for the particles as

$$\frac{d\boldsymbol{p}_i}{dt} = -\frac{\partial U\left(\{\boldsymbol{r}_j\}_{j=1}^N\right)}{\partial \boldsymbol{r}_i} - \zeta\frac{\boldsymbol{p}_i}{m} + \boldsymbol{\xi}_i(t), \tag{1}$$

where $\boldsymbol{\xi}_i = (\xi_i^x,\xi_i^y,\xi_i^z)$ represents thermal noise satisfying $\langle\xi_i^\alpha(t)\xi_j^\beta(t')\rangle = 2\zeta k_{\rm B}T\delta_{ij}\delta^{\alpha\beta}\delta(t-t')$, $k_{\rm B}$ is the Boltzmann constant, T is the temperature of the solvent, and ζ is the friction coefficient. The superscripts α and β represent Cartesian components. (See Ref. [10].) In numerical simulations, all the quantities are converted to dimensionless forms by setting $m = \sigma = \epsilon = 1$. We fix $T = 1.5$, $\zeta/k_{\rm B}T = 1$, $N = 1024$, $r_{\rm c} = 2.5\sigma$, and $r^* = 0.5\sigma$, and treat ρ and $\dot{\gamma}^{\rm ex}$ as control parameters. We discretize (1) according to the reversible system propagator algorithm [11] with time step $\Delta t = 1/256$.

In this paper, $\langle \dots \rangle$ represents the statistical average in steady states.

III. ORDER PARAMETERS

We define an order parameter that characterizes a rotational symmetry breaking [12,13]. Using the Delaunay triangular decomposition [14] on a particle configuration, we determine neighboring particles for a given particle i. The collection of edges that extend from $\boldsymbol{r}_i$ in the Delaunay triangular is denoted by $(\boldsymbol{r}_{ij})_{j=1}^{n_{\rm B}(i)}$, where $n_{\rm B}(i)$ represents the number of neighbors of particle i. From this collection, we define a 13-dimensional vector $\boldsymbol{q}_6(i) = [q_{6,-6}(i), \dots, q_{6,m}(i), \dots q_{6,6}(i)]$ as

$$q_{6,m}(i) = \frac{1}{n_{\rm B}(i)} \sum_{j=1}^{n_{\rm B}(i)} Y_{6,m}\left(\frac{\boldsymbol{r}_{ij}}{|\boldsymbol{r}_{ij}|}\right), \tag{2}$$

where $Y_{6,m}$ is the spherical harmonics function of degree six. Then, the bond-orientational order is qualified by $\bar{q}_{6,m} = 1/N \sum_{i=1}^{N} q_{6,m}(i)$, where $\langle \bar{q}_{6,m} \rangle = 0$ if the rotational symmetry is not broken, while $\langle \bar{q}_{6,m} \rangle \neq 0$ in the thermodynamic limit $N \to \infty$ when the bond-orientational order emerges. In order to detect symmetry breaking, it is convenient to measure the magnitude of the vector $\bar{q}_{6,m}$. Following the standard convention, we define

$$Q_6 \equiv \left\langle \left(\frac{4\pi}{13} \sum_{m=-6}^{6} \bar{q}_{6,m} \bar{q}^*_{6,m} \right)^{1/2} \right\rangle. \tag{3}$$

Note that $Q_6 \simeq O(1/\sqrt{N})$ in the disordered phase, while $Q_6 \simeq O(1)$ in the ordered phase, when $N \to \infty$.

On the left-hand side of Fig. 1, we show Q_6 as a function of ρ for several values of $\dot{\gamma}^{\rm ex}$. The figure indicates the existence of an ordered state with $Q_6 \simeq O(1)$ in a high-density regime for each $\dot{\gamma}^{\rm ex}$. In particular, the transition to the ordered phase is quite sharp when $\dot{\gamma}^{\rm ex} = 0$, while the transition width becomes wider as $\dot{\gamma}^{\rm ex}$ is increased. For a tentative value of the transition point, we define $\rho_{\rm q}$ as the density such that $Q_6 = 0.2$. We display $\rho_{\rm q}$ as a function of $\dot{\gamma}^{\rm ex}$ in the right-hand side of Fig. 1. More precise determination of the functional forms of Q_6 will be obtained by investigating larger systems. Note that, in the thermodynamic limit without shear flow, nonzero Q_6 emerges continuously for a density at which a crystal can coexist with a liquid. When we ignore the coexistence phase, Q_6 exhibits a discontinuous transition, which is observed for the system under constant pressure. In this paper, putting aside phenomena associated with the coexistence phase, we focus

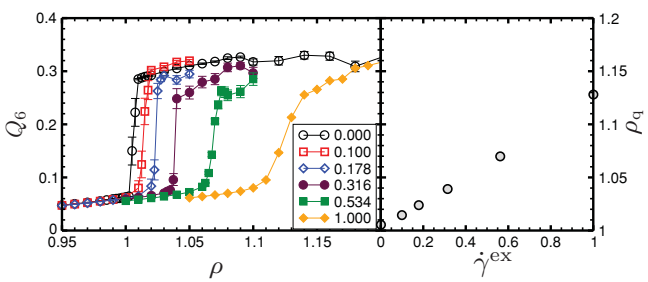

FIG. 1. (Color online) Left: Q_6 as a function of ρ for several values of $\dot{\gamma}^{\rm ex}$. Right: $\rho_{\rm q}$ as a function of $\dot{\gamma}^{\rm ex}$.

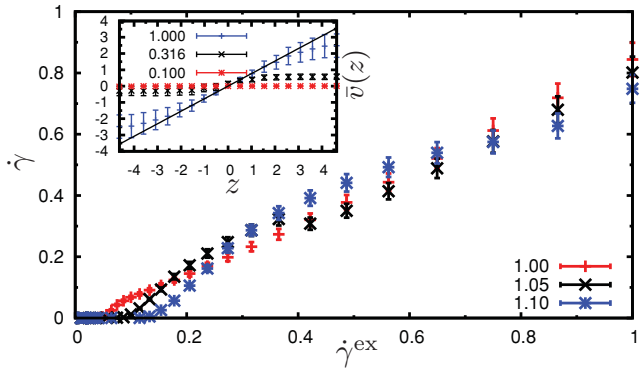

FIG. 2. (Color online) Shear rate of particle flow as a function of $\dot{\gamma}^{\rm ex}$ for several values of ρ. Each point is obtained from the velocity profiles $\bar{v}(z)$. Examples of velocity profiles for different $\dot{\gamma}^{\rm ex}$ with $\rho = 1.1$ fixed are shown in the inset.

on the question of how the nature of the symmetry-breaking discontinuous-transition is modified by the influence of shear flow.

In the equilibrium case, the ordered phase corresponds to a crystal. However, in the nonequilibrium cases, since the shear flow drives particles, particles may flow even in the ordered phase with $Q_6 \neq 0$. We then measure the x component of the velocity averaged over a region with an interval $[z + 0.5, z - 0.5]$ in the z direction, which is denoted by $\bar{v}(z)$. Examples of $\bar{v}(z)$ for several values of $\dot{\gamma}^{\rm ex}$ with $\rho = 1.1$ fixed are shown in the inset of Fig. 2. We then determine the shear rate $\dot{\gamma}$ of particles by fitting the slope of the velocity profile $\bar{v}(z)$ in the region $-1.5 < z < 1.5$. The obtained shear rates $\dot{\gamma}$ are plotted for $\dot{\gamma}^{\rm ex}$ in Fig. 2. Although the flow might cease at some value of $\dot{\gamma}^{\rm ex}$, the determination as to whether the crossover is actually singular is a delicate problem. (See Ref. [15] for a related discussion.) For any case, the crossover points are located at a higher density than $\rho_{\rm q}$ when $\dot{\gamma}^{\rm ex} > 0$ (see Fig. 3). Therefore, as we are concerned with behaviors near the transition point at which the order parameter $Q_6 \simeq O(1)$ appears, we may assume that an ordered fluid is observed in the ordered phase in the nonequilibrium cases.

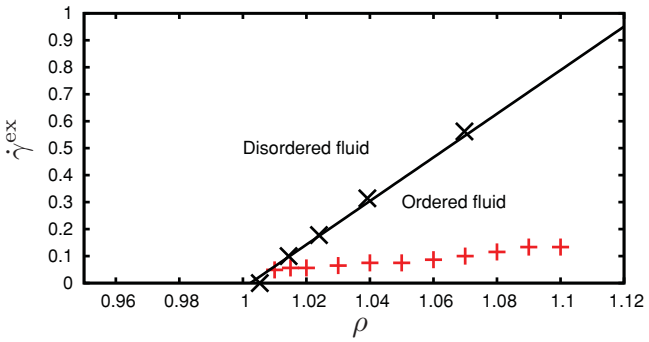

FIG. 3. (Color online) Phase diagram in the $(\rho, \dot{\gamma}^{\rm ex})$ plane. The cross symbols represent the transition line $\rho = \rho_{\rm q}(\dot{\gamma}^{\rm ex})$ between the disordered and the ordered fluid phases. The parameter values for realizing $\dot{\gamma} = 0.001$, below which flow appears to cease, are also plotted as plus symbols.

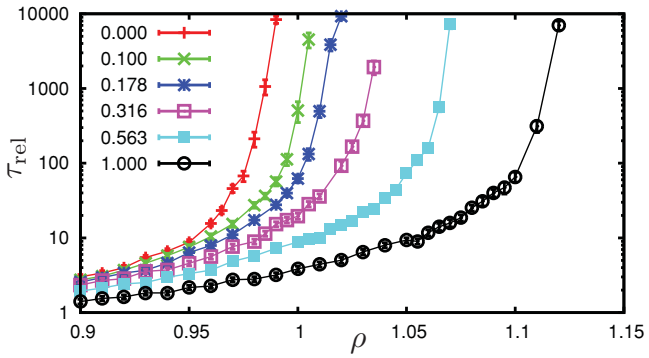

FIG. 4. (Color online) Relaxation time $\tau_{\rm rel}$ as a function of density ρ for several values of $\dot{\gamma}^{\rm ex}$.

IV. TRANSITION TO THE ORDERED FLUID

Next, we characterize the nature of the transition to the ordered phase. First, in order to observe a clear difference between the equilibrium and nonequilibrium cases, we measure the relaxation time $\tau_{\rm rel}$ at which Q_6 reaches a value of 0.05, starting from a crystal state, at which $Q_6 \approx 0.35$. Note that $\tau_{\rm rel}$ can be measured only in the disordered phase. In Fig. 4, we show $\tau_{\rm rel}$ as a function of ρ for several values of $\dot{\gamma}^{\rm ex}$, where we set the maximum waiting time to $\tau = 10\,000$. The results indicate the existence of a characteristic density $\rho_{\rm d}$ at which the relaxation time diverges for each value of $\dot{\gamma}^{\rm ex}$.

Let us determine the functional form of $\tau_{\rm rel}$ with the value of $\rho_{\rm d}$. First, as shown in the inset of Fig. 5, $\tau_{\rm rel}$ for the equilibrium case is well fitted by the Vogel-Fulcher law

$$\tau_{\rm rel} \simeq \tau_0 \exp\left(\frac{A}{\rho_{\rm d} - \rho}\right). \tag{4}$$

A phenomenological argument may be developed for the nucleation of a disordered domain, by which (4) may be understood. (See, for example, Ref. [8] for a demonstration of a q-states Potts model.) In contrast, Fig. 5 indicates that $\tau_{\rm rel}$ for the systems under shear flow follows a power-law form

$$\tau_{\rm rel} \simeq B(\dot{\gamma}^{\rm ex})[\rho_{\rm d}(\dot{\gamma}^{\rm ex}) - \rho]^{-\zeta}, \tag{5}$$

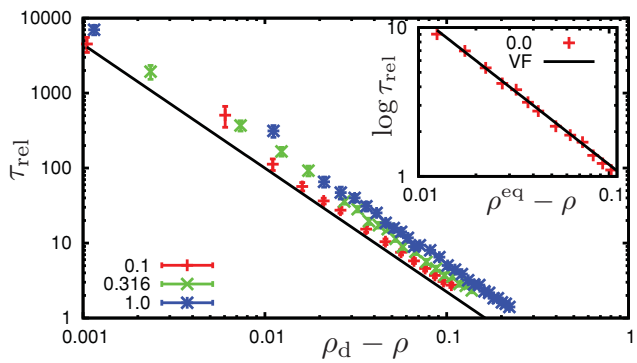

FIG. 5. (Color online) Fitting of functional forms of $\tau_{\rm rel}$. $\tau_{\rm rel}$ versus $\rho_{\rm d} - \rho$ with a log-log plot for $\dot{\gamma}^{\rm ex} = 0.1$, 0.316, and 1.0. $\rho_{\rm d}$ is a fitting parameter, the value of which is estimated as 1.006, 1.037, and 1.121, respectively. The guide line represents (5) with $\zeta = 1.6$. Inset: log $\tau_{\rm rel}$ versus $\rho_{\rm d} - \rho$ with a log-log plot for $\dot{\gamma}^{\rm ex} = 0$. The guide line represents (4) with $A = 0.1$ and $\rho_{\rm d} = 1.003$.

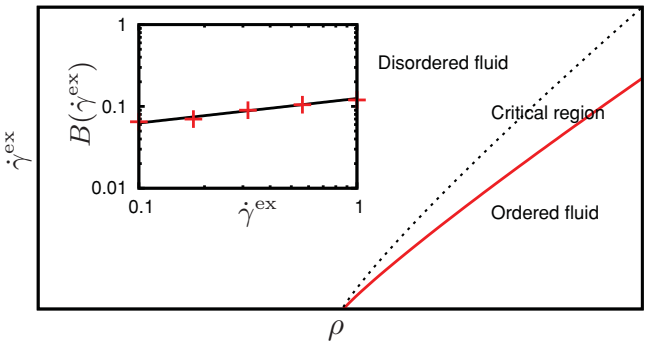

FIG. 6. (Color online) Schematic phase diagram with the critical region in the (ρ-$\dot{\gamma}^{\rm ex}$) plane. Inset: $B(\dot{\gamma}^{\rm ex})$ as a function of $\dot{\gamma}^{\rm ex}$. The guide line represents a power-law function with exponent 0.3.

where $\zeta \simeq 1.6$. This suggests that the divergent behavior does not originate from the nucleation of disordered regions but may be related to critical slowing down. Note that the prefactor B in (5) depends slightly on $\dot{\gamma}^{\rm ex}$ in the form $B \simeq (\dot{\gamma}^{\rm ex})^{0.3}$, as shown in the inset of Fig. 6. Let $\rho_{\rm w}(\dot{\gamma}^{\rm ex})$ be a typical width of the power-law region for $\dot{\gamma}^{\rm ex}$. Then, on the basis of the dimensional analysis, it is expected that

$$\dot{\gamma}^{\rm ex}\tau_{\rm rel} \simeq \left(\frac{\rho_{\rm d}(\dot{\gamma}^{\rm ex}) - \rho}{\rho_{\rm w}}\right)^{-\zeta}. \tag{6}$$

By assuming $\rho_{\rm w} \simeq (\dot{\gamma}^{\rm ex})^{\chi}$ in (6), we obtain $B \simeq (\dot{\gamma}^{\rm ex})^{\chi\zeta - 1}$, which leads to $\chi \simeq 1.3/1.6 > 0$. This means that a critical region for the system with finite $\dot{\gamma}^{\rm ex}$ becomes narrower for smaller $\dot{\gamma}^{\rm ex}$ and vanishes in the equilibrium system. See the schematic phase diagram in Fig. 6.

We now note that such a divergent time scale is never observed in the stationary state of the equilibrium system. In order to confirm this explicitly, we measure the time correlation function defined by

$$C(t) = \sum_{m=-6}^{6} [\langle \bar{q}_{6,m}(t_0)\bar{q}^*_{6,m}(t_0 + t)\rangle - \langle \bar{q}_{6,m}\rangle^2]. \tag{7}$$

We determine the correlation time $\tau_{\rm c}$ from the fitting of the exponential decay rate of $C(t)$. On the left-hand side of Fig. 7, $\tau_{\rm c}$ is shown as a function of ρ in the disordered regime. Indeed, the correlation time does not diverge. For reference, we superimpose the data of the relaxation time $\tau_{\rm rel}$. In contrast to

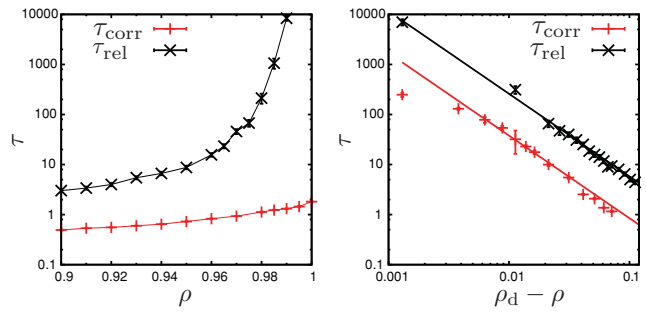

FIG. 7. (Color online) Correlation time $\tau_{\rm corr}$ in steady states as a function of ρ. The melting time $\tau_{\rm rel}$ is also superimposed for comparison. Left: $\dot{\gamma}^{\rm ex} = 0$. Right: $\dot{\gamma}^{\rm ex} = 1$.

the equilibrium case, as shown in the right-hand side of Fig. 7, the correlation time in the system under shear flow diverges in a manner similar to $\tau_{\rm rel}$. These results indicate that the symmetry-breaking transition to the ordered fluid accompanies a critical phenomenon. This is the main claim of this paper.

V. CONCLUDING REMARKS

Before ending this paper, we address five considerations. First, we conjecture that the fluctuation of $\boldsymbol{q}_6$ possesses a divergent length scale. By investigating the manner of divergences of several quantities for systems of different sizes, the universality class for this phenomenon may be determined.

Second, with regard to the universality problem, we are also interested in a simple mathematical model in the same universality class. For example, it might be possible to propose a model describing a stochastic time evolution of the coarse-grained order-parameter field. The first problem in this direction is to derive the value of ζ using a phenomenological argument.

Third, in all of the arguments presented above, the coexistence phase is ignored. To extract more precise results, it might be better to investigate systems under constant pressure. A study of such systems of larger sizes will be performed in future.

Fourth, the mechanism of the criticality remains to be clarified. Among several possibilities for the mechanism, which includes gelation of locally crystalline structure and change in order of the transition induced by an external force as discussed in Ref. [16], we wish to determine the true scenario. To do it, we will investigate the cooperative dynamics of locally crystalline clusters near the transition point.

Last, but not least, it is stimulating to observe the shear-induced criticality in laboratory experiments. Related to this subject, we note that, quite recently, Q_6 has been measured by direct observation of particles' configuration with using confocal microscopy under shear flow [17]. We hope that the shear-induced criticality will be investigated theoretically and experimentally.

ACKNOWLEDGMENTS

We thank M. Kobayashi for discussions on the role of the order parameters $\bar{q}_{6,m}$. This study was supported by grants from the Ministry of Education, Culture, Sports, Science, and Technology of Japan (Grants No. 21015005 and No. 22340109), and by a grant-in-aid from JSPS (DC2) (Grant No. 21-10700, 2009).

[1] B. J. Ackerson and N. A. Clark, Phys. A (Amsterdam) **110**, 221 (1983); Phys. Rev. A **30**, 906 (1984).

[2] S. Butler and P. Harrowell, J. Chem. Phys. **103**, 4653 (1995); **105**, 605 (1996).

[3] P. Holmqvist, M. P. Lettinga, J. Buitenhuis, and J. K. G. Dhont, Langmuir **21**, 10976 (2005).

[4] S. Butler and P. Harrowell, Nature (London) **415**, 1008 (2002); J. Chem. Phys. **118**, 4115 (2003); Phys. Rev. E **67**, 051503 (2003).

[5] R. Blaak, S. Auer, D. Frenkel, and H. Löwen, Phys. Rev. Lett. **93**, 068303 (2004).

[6] M. J. Miyama and S. I. Sasa, J. Phys. Condens. Matter **20**, 035104 (2008).

[7] L. D. Landau and E. M. Lifshitz, *Statistical Physics*, 3rd ed. (Butterworth-Heinemann, Oxford, 1980).

[8] F. Krzakala and L. Zdeborová, J. Chem. Phys. **134**, 034512 (2011).

[9] J. D. Weeks, D. Chandler, and H. C. Andersen, J. Chem. Phys. **54**, 5273 (1971).

[10] M. G. McPhie, P. J. Daivis, I. K. Snook, J. Ennis, and D. J. Evans, Phys. A (Amsterdam) **299**, 412 (2001).

[11] M. Tuckerman, B. J. Berne, and G. J. Martyna, J. Chem. Phys. **97**, 1990 (1992); G. Bussi and M. Parrinello, Phys. Rev. E **75**, 056707 (2007).

[12] P. J. Steinhardt, D. R. Nelson, and M. Ronchetti, Phys. Rev. B **28**, 784 (1983); J. S. van Duijneveldt and D. Frenkel, J. Chem. Phys. **96**, 4655 (1992).

[13] U. Gasser, E. R. Weeks, A. Schofield, P. N. Pusey, and D. A. Weitz, Science **292**, 258 (2001); J. Hernández-Guzmán and E. R. Weeks, Proc. Natl. Acad. Sci. USA **106**, 15198 (2009).

[14] D. C. Rapaport, *The Art of Molecular Dynamics Simulation,* 2nd ed. (Cambridge University Press, Cambridge, England, 2004).

[15] F. Sausset, G. Biroli, and J. Kurchan, J. Stat. Phys. **140**, 718 (2010).

[16] A. Chowdhury, B. J. Ackerson, and N. A. Clark, Phys. Rev. Lett. **55**, 833 (1985); J. Chakrabarti, H. R. Krishnamurthy, and A. K. Sood, *ibid.* **73**, 2923 (1994).

[17] L. T. Shereda, R. G. Larson, and M. J. Solomon, Phys. Rev. Lett. **105**, 228302 (2010).